research article

Identification of differentially expressed genes associated with the enhancement of X-ray susceptibility by RITA in a hypopharyngeal squamous cell carcinoma cell line (FaDu)

Jinwei Luan, Xianglan Li, Rutao Guo, Shanshan Liu, Hongyu Luo, Qingshan You

Department of Radiation Oncology, The Third Affiliated Hospital of Harbin Medical University, Harbin, China

Correspondence to: Qingshan You, M.D., Department of Radiation Oncology, The Third Affiliated Hospital of Harbin Medical University, Num.150, Haping Road, Harbin, China, 150081. Phone and Fax: +860 451 8629 8532; E-mail: haveqingsh@163.com

Background. Next generation sequencing and bio-informatic analyses were conducted to investigate the mechanism of reactivation of p53 and induction of tumor cell apoptosis (RITA)-enhancing X-ray susceptibility in FaDu cells.

Materials and methods. The cDNA was isolated from FaDu cells treated with 0 X-ray, 8 Gy X-ray, or 8 Gy X-ray + RITA. Then, cDNA libraries were created and sequenced using next generation sequencing, and each assay was repeated twice. Subsequently, differentially expressed genes (DEGs) were identified using Cuffdiff in Cufflinks and their functions were predicted by pathway enrichment analyses. Genes that were constantly up- or down-regulated in 8 Gy X-ray-treated FaDu cells and 8 Gy X-ray + RITA-treated FaDu cells were obtained as RITA genes. Afterward, the protein-protein interaction (PPI) relationships were obtained from the STRING database and a PPI network was constructed using Cytoscape. Furthermore, ClueGO was used for pathway enrichment analysis of genes in the PPI network.

Results. Total 2,040 and 297 DEGs were identified in FaDu cells treated with 8 Gy X-ray or 8 Gy X-ray + RITA, respectively. *PARP3* and *NEIL1* were enriched in base excision repair, and *CDK1* was enriched in p53 signaling pathway. *RFC2* and *EZH2* were identified as RITA genes. In the PPI network, many interaction relationships were identified (e.g., RFC2-CDK1, EZH2-CDK1 and PARP3-EZH2). ClueGO analysis showed that *RFC2* and *EZH2* were related to cell cycle.

Conclusions. *RFC2*, *EZH2*, *CDK1*, *PARP3* and *NEIL1* may be associated, and together enhance the susceptibility of FaDu cells treated with RITA to the deleterious effects of X-ray.

Key words: hypopharyngeal squamous cell carcinoma; next generation sequencing; RITA; X-ray

Introduction

Head and neck squamous cell carcinoma (HNSCC), which arises in the head and neck region that composes pharynx, larynx, nasal cavity, oral cavity, paranasal sinuses and salivary glands, has an estimated 500,000 new cases and becomes the sixth most common cancer in 2010 worldwide.[1] As one type of HNSCC, hypopharyngeal squamous cell carcinoma (HSCC) has a poor prognosis, and the overall survival rate for HSCC patients is only 15–45%.[2,3] The patients diagnosed with HSCC are often at a late stage and distant metastasis occur after conventional treatments.[2] Thus, the poor survival of patients with HSCC may be due to lacking of early detection and highly metastatic behavior.[4] Radiotherapy is the principal treatment of loco-regionally advanced squamous-cell carcinoma of the head and neck region (including oral cavity, oropharynx, hypopharynx, and larynx).[5,6] Recently, instead of radiotherapy, chemoradiotherapy has become the standard treatment for patients with locally advanced disease.[7] Many small molecules have

been identified to enhance the radiation response. For example, panitumumab has been discovered to have an enhanced effect on radiation in the preclinical setting of upper aerodigestive tract cancer.[8] Moreover, it has been found that the p53-reactivating small-molecule RITA (reactivation of p53 and induction of tumor cell apoptosis), alone or in combination with cisplatin, can induce the reactivation of *p53* in many HNSCC cell lines.[9,10] However, this effect is not universal. The HNSCC cell line JHU-028 can express wild type (wt) *p53*, but the cells do not undergo apoptosis in response to RITA treatment.[10]

Previously, we used RITA combined with X-ray to investigate the effect of RITA on X-ray susceptibility for the treatment of HSCC cell line FaDu (which is HPV-negative cell line) and found that RITA could enhance the radiation response of HSCC (data not shown). In this study, using RNA sequencing data from the HSCC cell line FaDu, we aimed to screen differentially expressed genes (DEGs) between 8 Gy X-ray-treated FaDu cells and 0 Gy X-ray-treated FaDu cells, as well as those between 8 Gy X-ray + RITA treated FaDu cells and 8 Gy X-ray treated FaDu cells. The underlying functions of the DEGs were predicted by Gene Ontology (GO), Kyoto Encyclopedia of Genes and Genomes (KEGG) and BioCarta enrichment analysis. Moreover, the genes related to RITA were further analyzed. Additionally, a protein-protein interaction (PPI) network was constructed to identify key genes involved in enhanced X-ray susceptibility of FaDu cells treated with RITA.

Materials and methods

Cell culture and processing

The HSCC cell line FaDu was purchased from American Type Culture Collection (ATCC, Manassas, VA, USA). The FaDu cells were cultured in media made from Dulbecco modified Eagle medium (DMEM, GIBCO, Gaithersburg, USA), 10% fetal bovine serum (FBS, GIBCO) and 1% mycillin double antibody (GIBCO) at 37°C in a humidified, 5% CO_2 incubator (Thermo, Pittsburgh, USA). When the confluency of FaDu cells covered 80%-90% of the petri dish, they were digested with pancreatin (GIBCO), centrifuged, and the supernatant was discarded. Next, the FaDu cells were resuspended in a frozen stock solution composed of 10% dimethyl sulfoxide (DMSO, GIBCO), 40% FBS and 50% DMEM, and preserved in a program frozen box.

After digestion, FaDu cells were centrifuged and counted, and then inoculated in 96-well plates (ABI, Foster City, USA) ($6×10^4$ cells/well) and cultured overnight. Subsequently, RITA (10 μM) (Selleck, Houston, USA) was added to each well of the experimental group, and DMSO (0.1%) was added to that the wells of the control group. The cells were preprocessed for 24 h at 37°C in a humidified, 5% CO_2 incubator. The plates were then sealed by parafilm and placed in a radiometer, and the cells in the experimental group were irradiated with a radiation dose of 8 Gy and a radiation speed of 1 Gy/min. After irradiation, the parafilm was removed and the plates were placed at 37°C in a humidified, 5% CO_2 incubator for 48 h.

RNA isolation and sequencing preparation

The total RNA was extracted from the cells using the SV total RNA Isolation System (Invitrogen, Shanghai, CHN) according to the manufacturer's instructions. The integrity of the total RNA was verified by 2% Agarose Gel Electrophoresis. The purity of RNA was determined by the A260/A280 ratio as determined by a spectrophotometer (Merinton, Beijing, CHN).

Construction of cDNA library

The cDNA libraries were constructed using a NEBNext® Ultra™ RNA Library Prep Kit for Illumina® (NEB E7530) (Vazyme, Nanjing, CHN), according to the manufacturer's instructions. Through heating, mRNA was broken into short fragments (200 nt). Using these short fragments as templates, random hexamer-primer (Sangon, Shanghai, CHN) was used to synthesize the first-strand of cDNA. Next, the second-strand of cDNA was synthesized. The short fragments were connected to sequencing adapters after poly (A) sequences were added. Afterwards, the UNG enzyme (Prospect Biosystems, Newark, USA) was used to degrade the second-strand cDNA, and the product was purified using a MiniElute PCR Purification Kit (Qiagen, Dusseldorf, GER) before PCR amplification. Finally, the library could be sequenced using an Illumina Hiseq 2500 v4 100PE (Illumina, San Diego, USA), and raw reads were generated. Reads with adaptor sequences, with unknown nucleotide content higher than 10% and/or those with low quality bases accounting for higher than 50% of the total nucleotides were filtered out.

Sequence alignment and identification of differentially expressed genes

The high quality reads were mapped to the human genome (version: hg19) using Tophat (version: 2.0.12), and BAM files were obtained.[11] The parameters were set to defaults. Cuffdiff in Cufflinks[12] was used to identify DEGs. The Benjamini & Hochberg method[13] was applied to correct for multiple tests. The adjusted p-value (that is false discovery rate, FDR) < 0.05 and |log fold change (FC)| ≥ 1 were used as the cut-off criteria.

Functional enrichments

The KEGG pathway database can be used to identify the relationships and interactions between genes in a given system.[14] KEGG was used for pathway enrichment analysis, and a p-value < 0.05 was considered a significantly enriched pathway.

The genes related to RITA (RITA genes) screening

To further investigate the effect of RITA on FaDu cells, we identified common DEGs in 0 Gy X-ray treated FaDu cells vs 8 Gy X-ray treated FaDu cells, and 8 Gy X-ray treated FaDu cells vs 8 Gy X-ray + RITA treated FaDu cells (Figure 1). A previous study showed that X-rays could reduce cell viability and that treatment with RITA could enhance the susceptibility of FuDa cells to the deleterious effects of X-rays.[10] Therefore, the genes that were consistently up- or down-regulated in 8 Gy X-ray treated FaDu cells vs 0 Gy X-ray treated FaDu cells and 8 Gy X-ray + RITA treated FaDu cells vs 8 Gy X-ray treated FaDu cells were characterized as the RITA genes.

PPI network construction

The online tool STRING[15] was utilized to analyze the interactions between the proteins encoded by the common DEGs. A required confidence (com-
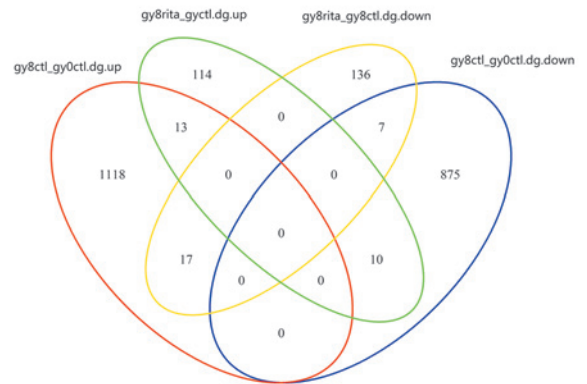
FIGURE 1. Venn diagram of DEGs between 0 GY X-ray-treated FaDu cells and 8 GY X-ray-treated FaDu cells, as well as the DEGs between 8 GY X-ray-treated FaDu cells and 8 GY X-ray + RITA-treated FaDu cells.

bined score) > 0.4 was used as the cut-off criterion. Subsequently, Cytoscape software[16] was used to visualize the PPI network.

ClueGO analysis

ClueGO[17] in Cytoscape was used to conduct GO, KEGG and BioCarta enrichment analyses. Further, ClueGO divided terms into different functional groups based on the common genes involved in different terms. In our study, ClueGO was used for KEGG pathway enrichment analysis. A p-value < 0.05 was used as the cut-off criterion.

# Results

Alignment analysis

The total reads were above 82% and the mapped reads were above 70% in all of the data sets. The detailed sequencing information is shown in Table 1.

DEG analysis

Compared with 0 Gy X-ray-treated FaDu cells, a total of 2,040 DEGs (1,148 up-regulated and 892

TABLE 1. Summary statistics of paired-end (PE) RNA-Seq reads in six cell lines

Sample	Total PE reads	Total high quality PE reads	Total mapped PE reads	Total uniquely mapped PE reads
Sample_L141211001	10467886	8650424 (82.3%)	6846290 (79.1%)	6749179
Sample_L141211002	11510210	9627883 (83.6%)	7197526 (74.7%)	7097908
Sample_L141211003	11119410	9365349 (84.2%)	6910499 (73.7%)	6825529
Sample_L141211004	11271934	9510517 (84.3%)	6752339 (70.9%)	6669811
Sample_L141211005	10854414	9110446 (83.9%)	7129465 (78.2%)	7043831
Sample_L141211006	10532245	8802840 (83.5%)	6752224 (76.7%)	6671073
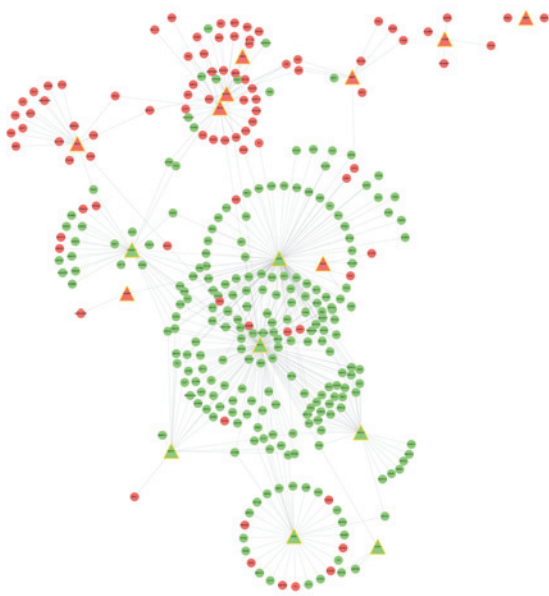
FIGURE 2. The PPI network for the RITA genes and their related DEGs. The red hubs represent the up-regulated DEGs; the green hubs represent the down-regulated DEGs; the triangle hubs represent the RITA genes; the lines represent the interactions between the genes.

down-regulated DEGs) were identified in the 8 Gy X-ray-treated FaDu cells. Moreover, 297 DEGs (137 up-regulated and 160 down-regulated DEGs) were identified in the 8 Gy X-ray + RITA-treated FaDu cells compared with the 8 Gy X-ray-treated FaDu cells.

Pathway enrichment analysis

The results of KEGG pathway enrichment for the DEGs are listed in Table 2. Replication factor C subunit 2 (*RFC2*) was significantly enriched in DNA replication (p = 5.85E-19) and nucleotide excision repair (p = 2.25E-04). Poly (ADP-ribose) polymerase 3 (*PARP3*) and nei endonuclease VIII-like 1 (*NEIL1*) were significantly enriched in the pathway of base excision repair (p = 2.00E-08). Moreover, cyclin-dependent kinase 1 (*CDK1*) was significantly enriched in the p53 signaling pathway (p = 1.85E-02).

RITA genes screening

A total of 20 consistently dysregulated genes in the 8 Gy X-ray-treated FaDu cells vs 0 Gy X-ray-

TABLE 2. The top ten up- and down-regulated DEGs between 0 GY X-ray treated FaDu cells and 8 GY X-ray treated FaDu cells, as well as 8 GY X-ray treated FaDu cells and 8 GY X-ray + RITA treated FaDu cells

	Gene symbols	log2 fold change	P-value	Gene symbols	log2 fold change	P-value
Up-regulated	BMF	-1.79769e+308	1.23E-11	BMF	-1.79769e+308	1.23E-11
	SDCBP	-1.79769e+308	0.00097112	SDCBP	-1.79769e+308	0.00097112
	IL32	-1.79769e+308	0.0110064	IL32	-1.79769e+308	0.0110064
	MAD1L1	-1.79769e+308	9.77E-05	MAD1L1	-1.79769e+308	9.77E-05
	SIRT3	-1.79769e+308	0.00289562	SIRT3	-1.79769e+308	0.00289562
	KAZN	-1.79769e+308	7.93E-10	KAZN	-1.79769e+308	7.93E-10
	TSPAN4	-1.79769e+308	0.0136997	TSPAN4	-1.79769e+308	0.0136997
	PPAN-P2RY11	-1.79769e+308	4.71E-08	PPAN-P2RY11	-1.79769e+308	4.71E-08
	CDC14B	-1.79769e+308	1.49E-06	CDC14B	-1.79769e+308	1.49E-06
	CXCL16	-1.79769e+308	0.000434357	CXCL16	-1.79769e+308	0.000434357
Down-regulated	C3orf14	-5.88442	0.006353	KCTD2	-3.8901	1.23E-06
	TTC28-AS1	-3.10554	1.30E-09	TSPAN4	-3.68234	0.0124825
	KRT4	-2.86398	0	FGFR3	-3.47603	0.0322468
	ALPP	-2.68741	1.30E-13	PLEKHM1.1	-3.41618	0.0191408
	MND1	-2.64752	0.022297	CHFR	-3.39824	0.0369514
	DHRS2	-2.38983	4.17E-11	KREMEN2	-3.32824	0.033903
	FGF3	-2.33156	2.25E-12	SMAP2	-3.3199	0.0215792
	TERC	-2.268	0.027132	EPS15L1	-3.30518	0.00562372
	UTP20	-2.23728	0	MORF4L2	-3.0731	0.0300806
	GAL	-2.22661	0	PIGQ	-2.94079	0.0327601

DEGs = differentially expressed genes
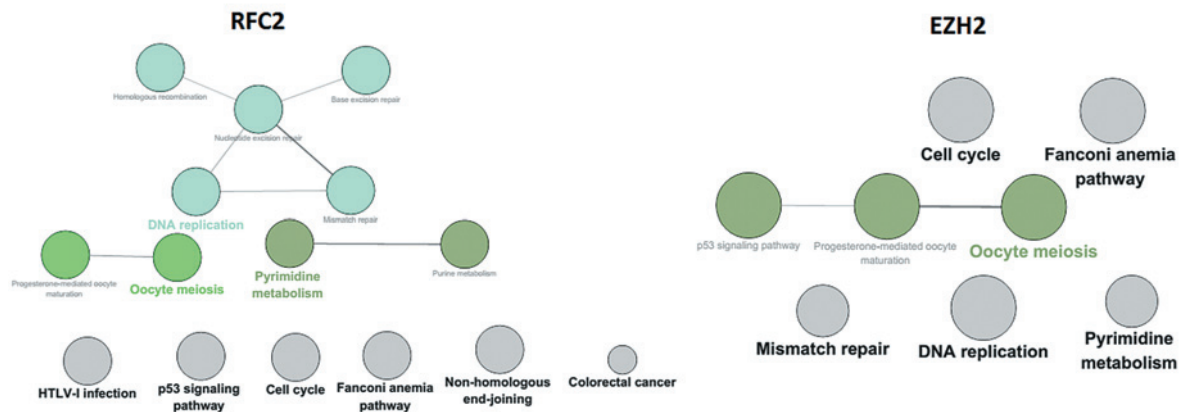
FIGURE 3. Functional annotation for *RFC2* and *EZH2* clusters. Node color represents the functional groups; node size reflects the p-value, with the smaller the node size indicating larger p-values, while the larger node size represents smaller p-values.

treated FaDu cells and in the 8 Gy X-ray + RITA-treated FaDu cells vs 8 Gy X-ray-treated FaDu cells were identified, including 13 consistently up-regulated (B cell lymphomas 6, *BCL6*; integrin, beta 2-antisense RNA 1, *ITGB2-AS1*; L1 cell adhesion molecule, *L1CAM*; LIM and calponin homology domains 1, *LIMCH1*; latent transforming growth factor-β binding protein 3, *LTBP3*; v-MAF avian musculoaponeurotic fibrosarcoma oncogene family, *MAFF*; neutrophil cytosolic factor 2, *NCF2*; nuclear factor of activated T-cells, cytoplasmic, calcineurin-dependent 1, *NFATC1*; *PARP3*; RAB43, member RAS oncogene family, *RAB43*; regulator of cell cycle, *RGCC*; Src homology 2 domain containing F, *SHF*; and troponin T type 1, *TNNT1*) and 7 consistently down-regulated DEGs (adenylosuccinate lyase, *ADSL*; enhancer of zeste homolog 2, *EZH2*; nudix-type motif 1, *NUDT1*; proteasome 26S subunit, non-ATPase 11, *PSMD11*; *RFC2*; Treacher Collins-Franceschetti syndrome 1, *TCOF1*; and X-ray repair cross-complementing group 3, *XRCC3*) (Figure 1).

PPI network and module analysis

The PPI network for RITA genes and the DEGs related to RITA had 448 interactions (Figure 2). In the PPI network, the RITA genes of RFC2 (degree = 126) and EZH2 (degree = 115) had relatively higher degrees. Additionally, RFC2 and EZH2 could interact with CDK1. The results of the pathway enrichment analysis for RFC2, EZH2 and their interaction genes are shown in Figure 3. RFC2 and EZH2 were enriched in the cell cycle pathways, oocyte meiosis, and DNA replication.

Discussion

In the present study, a total of 2,040 DEGs, including 1,148 up-regulated and 892 down-regulated DEGs, were identified in 8 Gy X-ray-treated FaDu cells, compared with 0 Gy X-ray-treated FaDu cells. Moreover, 297 DEGs, including 137 up-regulated and 160 down-regulated DEGs, were identified in 8 Gy X-ray + RITA-treated FaDu cells, compared with 8 Gy X-ray-treated FaDu cells. Among these DEGs, *EZH2* and *RFC2*, which were consistently down-regulated in 8 Gy X-ray-treated FaDu cells vs 0 Gy X-ray-treated FaDu cells and 8 Gy X-ray + RITA-treated FaDu cells vs 8 Gy X-ray-treated FaDu cells, were characterized as the RITA genes. A previous study has reported that enhancers of *EZH2*, which is the enzymatic component of the polycomb repressive complex 2, can regulate cell proliferation and differentiation during embryonic development.[18] Moreover, it has also been demonstrated that targeting *EZH2* can suppress cancer progression and recurrence by reversing oncogenic properties and stemness of tumor cells.[19] *RFC2*, belonging to the replication factor C family, has been implicated in nasopharyngeal carcinoma.[20] In our study, ClueGO analysis showed that *RFC2* and *EZH2* were related to the cell cycle. Cell cycle regulation by p53 is widely accepted as the major mechanism for tumor formation.[21] Therefore, we speculated that *RFC2* and *EZH2* may regulate the cancer cell proliferation of HSCC cells through the cell cycle pathway. According to the PPI network, both RFC2 and EZH2 could interact with CDK1, and the KEGG pathway enrichments showed that *CDK1* was significantly enriched in the *p53* sign-

TABLE 3. The KEGG pathway enrichment for the DEGs between 0 GY X-ray treated FaDu cells and 8 GY X-ray treated FaDu cells, as well as 8 GY X-ray treated FaDu cells and 8 GY X-ray + RITA treated FaDu cells.

Term	Count	P value	Gene symbols
gy8ctl vs. gy0ctl			
hsa03030: DNA replication	28	5.85E-19	POLA1, POLA2, RPA3, RPA1, PRIM1, RPA2, POLE4, MCM7, POLE3, FEN1
hsa04110: Cell cycle	43	1.91E-11	E2F1, E2F2, DBF4, PRKDC, PKMYT1, CHEK1, CDC45, MCM7, CDKN2B, CDKN2C …
hsa03430: Mismatch repair	16	1.15E-09	EXO1, SSBP1, MSH2, LIG1, MLH1, RPA3, RFC5, POLD3, RPA1, RPA2 …
hsa00240: Pyrimidine metabolism	32	2.00E-08	POLR2G, DTYMK, POLA1, CAD, POLA2, CMPK2, TK1, PRIM1, TYMS, POLE4 …
hsa03410: Base excision repair	16	2.06E-06	HMGB1, UNG, NEIL3, LIG1, POLE, NEIL1, POLD3, POLD4, POLE4, POLE3 …
hsa03440: Homologous recombination	14	3.36E-06	RAD51C, XRCC3, NBN, BLM, SSBP1, MRE11A, EME1, RPA3, RAD51, POLD3 …
hsa03420: Nucleotide excision repair	15	2.25E-04	LIG1, POLE, RPA3, RFC5, POLD3, RPA1, RPA2, POLD4, RFC3, POLE4 …
hsa00230: Purine metabolism	33	3.73E-04	XDH, POLR2G, POLA1, POLA2, PFAS, PRIM1, POLE4, POLE3, PDE4A, ENTPD8 …
hsa05200: Pathways in cancer	52	0.010417112	FGF19, E2F1, HSP90AB1, E2F2, PTGS2, PDGFB, PGF, STAT5A, ARNT2, FGF11 …
hsa05219: Bladder cancer	11	0.016627297	E2F1, E2F2, TYMP, CDKN1A, PGF, VEGFA, RB1, DAPK2, CDK4, MMP2, DAPK1
hsa04115: p53 signaling pathway	15	0.018499656	CDK1, CYCS, CHEK1, ATR, CDK4, CCNG2, GTSE1, CCNB1, CDKN1A, CCNB2 …
hsa04512: ECM-receptor interaction	17	0.024887625	HSPG2, SDC4, COL5A1, CHAD, HMMR, VWF, LAMB3, LAMB2, ITGB8, ITGA5 …
hsa03020: RNA polymerase	8	0.03298698	POLR3G, POLR2G, POLR3K, POLR1E, POLR1A, POLR1C, POLR1B, POLR3B
hsa00970: Aminoacyl-tRNA biosynthesis	10	0.036943456	IARS, NARS2, LARS, FARSB, EPRS, WARS2, DARS2, AARS2, KARS, EARS2
hsa03040: Spliceosome	22	0.044130211	NCBP1, MAGOH, TRA2B, LSM6, TRA2A, SNRPD1, HSPA1A, PRPF4, RBMX, HNRNPA1 …
hsa05222: Small cell lung cancer	16	0.048720159	E2F1, TRAF1, E2F2, CKS1B, PTGS2, PIK3CD, CYCS, SKP2, RB1, BIRC3 …
gy8rita vs. gy8ctl			
hsa03410: Base excision repair	4	0.014381142	NEIL1, LIG3, PARP3, SMUG1
hsa05212: Pancreatic cancer	5	0.021107952	AKT1, PGF, PIK3CB, ERBB2, RALGDS
hsa05213: Endometrial cancer	4	0.040674333	AKT1, PIK3CB, ERBB2, CTNNA1
hsa04150: mTOR signaling pathway	4	0.040674333	AKT1, PGF, PIK3CB, EIF4E2

DEGs = differentially expressed genes

aling pathway. *p53* can negatively regulate the transcription of a large number of genes (including *BCL-2* and *MCL1*) that suppress apoptosis.[22] Additionally, a former study has also demonstrated that the reactivation of *p53* can induce apoptosis in HNSCC, which includes HSCC.[23] Consequently, we proposed that *CDK1* could be correlated with HSCC by regulation of apoptosis of the cancer cells through the *p53* signaling pathway. In addition, CDK1 might also function in HSCC through interacting with RFC2 and EZH2.

Additionally, the RITA gene *PARP3* was significantly enriched in base excision repair. Base excision repair is a cellular mechanism that repairs damaged DNA throughout the cell cycle. It has been reported that the DNA repair capacity is crucial for preventing genomic instability and, in turn, may be associated with heightened risk of cancer.[24] Furthermore, reduced expression of nucleotide excision repair core genes such as Cockayne's

syndrome complementary group B/excision repair cross-complementing 6 (*CSB/ERCC6*), excision repair cross-complementing 1 (*ERCC1*), Xeroderma pigmentosum group G/excision repair cross-complementing 5 (*XPG/ERCC5*) and Xeroderma pigmentosum group B/excision repair cross-complementing 3 (*XPB/ERCC3*) can increase the risk for development of HNSCC for more than two-fold.[25] The ADP ribosyl transferase *PARP3* gene has been identified as a vital player in the stabilization of mitotic spindles and in telomere integrity. Notably, *PARP3* associates and regulates the mitotic components NuMA and tankyrase 1; therefore, *PARP3* can be a potential biomarker in cancer therapy.[26] In the PPI network, PARP3 is capable of interacting with EZH2. Accordingly, it came to the speculation that PARP3, as well as its interaction with EZH2, could play a role in HSCC by regulating DNA damage through the base excision repair pathway. Moreover, *NEIL1* was also enriched in base exci-

sion repair. A former study showed that the functional variants of the NEIL1 protein can lead to risk and progression of squamous cell carcinomas of the oral cavity and oropharynx.[27] Therefore, *PARP3* and *NEIL1* could be involved in development of HSCC through the base excision repair pathway.

RFC2, EZH2, CDK1, PARP3 and *NEIL1* may be related to an enhancement of the susceptibility of FaDu cells to X-rays with co-treatment of RITA. However, further research is needed to illustrate their mechanisms.

References

1. Torre LA, Bray F, Siegel RL, Ferlay J, Lortet-Tieulent J, Jemal A. Global cancer statistics, 2012. *CA Cancer J Clin* 2015; **65:** 87-108.

2. Chaturvedi AK, Engels EA, Pfeiffer RM, Hernandez BY, Xiao W, Kim E, et al. Human papillomavirus and rising oropharyngeal cancer incidence in the United States. *J Clin Oncol* 2011; **29:** 4294-301.

3. Van Monsjou HS, Balm AJ, Van den Brekel MM, Wreesmann VB. Oropharyngeal squamous cell carcinoma: a unique disease on the rise? *Oral Oncol* 2010; **46:** 780-5.

4. Garden AS, Asper JA, Morrison WH, Schechter NR, Glisson BS, Kies MS, et al. Is concurrent chemoradiation the treatment of choice for all patients with Stage III or IV head and neck carcinoma? *Cancer* 2004; **100:** 1171-8.

5. Kramer S, Gelber RD, Snow JB, Marcial VA, Lowry LD, Davis LW, et al. Combined radiation therapy and surgery in the management of advanced head and neck cancer: final report of study 73–03 of the Radiation Therapy Oncology Group. *Head Neck Surg* 1987; **10:** 19-30.

6. Kato K, Muro K, Minashi K, Ohtsu A, Ishikura S, Boku N, et al. Phase II study of chemoradiotherapy with 5-fluorouracil and cisplatin for stage II–III esophageal squamous cell carcinoma: JCOG Trial (JCOG 9906). *Int J Radiat Oncol Biol Phys* 2011; **81:** 684-90.

7. Kruser TJ, Armstrong EA, Ghia AJ, Huang S, Wheeler DL, Radinsky R, et al. Augmentation of radiation response by panitumumab in models of upper aerodigestive tract cancer. *Int J Radiat Oncol Biol Phys* 2008; **72:** 534-42.

8. Roh J-L, Ko JH, Moon SJ, Ryu CH, Choi JY, Koch WM. The p53-reactivating small-molecule RITA enhances cisplatin-induced cytotoxicity and apoptosis in head and neck cancer. *Cancer Lett* 2012; **325:** 35-41.

9. Roh J-L, Kang SK, Minn I, Califano JA, Sidransky D, Koch WM. p53-Reactivating small molecules induce apoptosis and enhance chemotherapeutic cytotoxicity in head and neck squamous cell carcinoma. *Oral Oncol* 2011; **47:** 8-15.

10. Kim D, Pertea G, Trapnell C, Pimentel H, Kelley R, Salzberg SL. TopHat2: accurate alignment of transcriptomes in the presence of insertions, deletions and gene fusions. *Genome Biol* 2013; **14:** R36.

11. Trapnell C, Williams BA, Pertea G, Mortazavi A, Kwan G, van Baren MJ, et al. Transcript assembly and quantification by RNA-Seq reveals unannotated transcripts and isoform switching during cell differentiation. *Nat Biotechnol* 2010; **28:** 511-15.

12. Benjamini Y, Hochberg Y. Controlling the false discovery rate: a practical and powerful approach to multiple testing. *J R Stat Soc Series B Stat Methodol* 1995; **57:** 289-300.

13. Kanehisa M, Goto S. KEGG: kyoto encyclopedia of genes and genomes. *Nucleic Acids Res* 2000; **28:** 27-30.

14. Franceschini A, Szklarczyk D, Frankild S, Kuhn M, Simonovic M, Roth A, et al. STRING v9. 1: protein-protein interaction networks, with increased coverage and integration. *Nucleic Acids Res* 2013; **41:** D808-D15.

15. Saito R, Smoot ME, Ono K, Ruscheinski J, Wang P-L, Lotia S, et al. A travel guide to Cytoscape plugins. *Nat Methods* 2012; **9:** 1069-76.

16. Bindea G, Mlecnik B, Hackl H, Charoentong P, Tosolini M, Kirilovsky A, et al. ClueGO: a Cytoscape plug-in to decipher functionally grouped gene ontology and pathway annotation networks. *Bioinformatics* 2009; **25:** 1091-93.

17. Qi W, Chan H, Teng L, Li L, Chuai S, Zhang R et al. Selective inhibition of Ezh2 by a small molecule inhibitor blocks tumor cells proliferation. *Proc Natl Acad Sci* 2012; **109:** 21360-65.

18. Chang C, Hung M. The role of EZH2 in tumour progression. *Br J Cancer* 2012; **106:** 243-47.

19. Xiong S, Wang Q, Zheng L, Gao F, Li J. Identification of candidate molecular markers of nasopharyngeal carcinoma by tissue microarray and in situ hybridization. *Med Oncol* 2011; **28:** 341-48.

20. Li T, Kon N, Jiang L, Tan M, Ludwig T, Zhao Y, et al. Tumor suppression in the absence of p53-mediated cell-cycle arrest, apoptosis, and senescence. *Cell* 2012; **149:** 1269-83.

21. Mirzayans R, Andrais B, Scott A, Murray D. New insights into p53 signaling and cancer cell response to DNA damage: implications for cancer therapy. *Biomed Res Int* 2012: 170325. doi: 10.1155/2012/170325.

22. Chuang H-C, Yang LP, Fitzgerald AL, Osman A, Woo SH, Myers JN, et al. The p53-Reactivating Small Molecule RITA Induces Senescence in Head and Neck Cancer Cells. *PLoS One* 2014; **9:** e104821.

23. de Boer JG. Polymorphisms in DNA repair and environmental interactions. *Mutat Res* 2002; **509:** 201-10.

24. Song X, Sturgis EM, Jin L, Wang Z, Wei Q, Li G. Variants in nucleotide excision repair core genes and susceptibility to recurrence of squamous cell carcinoma of the oropharynx. *Int J Cancer* 2013; **133:** 695-704.

25. Boehler C, Gauthier LR, Mortusewicz O, Biard DS, Saliou J-M, Bresson A, et al. Poly (ADP-ribose) polymerase 3 (PARP3), a newcomer in cellular response to DNA damage and mitotic progression. *Proc Natl Acad Sci* 2011; **108:** 2783-88.

26. Zhai X, Zhao H, Liu Z, Wang L-E, El-Naggar AK, Sturgis EM, et al. Functional variants of the NEIL1 and NEIL2 genes and risk and progression of squamous cell carcinoma of the oral cavity and oropharynx. *Clin Cancer Res* 2008; **14:** 4345-52.